THE SOCIETY OF NAVAL ARCHITECTS AND MARINE ENGINEERS
and
THE SHIP STRUCTURE COMMITTEE

Paper presented at the Ship Structures Symposium '93
Sheraton National Hotel, Arlington, Virginia, November 16-17, 1993

Time Variant Reliability Analysis of a Mobile Offshore Unit

W. B. (Bill) Shi[1] and Paul A. Frieze[2]

[1]BMT Cortec, Wallsend Research Station, Wallsend, Tyne & Wear, United Kingdom
[2]Paul A Frieze & Associates, Strawberry Hill, Twickenham, United Kingdom

Abstract

A time invariant structural reliability analysis of a mobile offshore unit was the central theme of the report of the Applied Design Committee of the 11th International Ship and Offshore Structures Congress. This paper makes use of the available structural and hydrodynamic data on the unit to demonstrate the effects on vessel structural integrity of in-service defects, primarily localized corrosion wastage. Results from this time variant reliability analysis are compared with those reported in the 11th ISSC. The findings from the investigation highlight the importance of the life cycle design philosophy for ships and offshore structures alike.

Introduction

The Applied Design Committee report of the 11th International Ship and Offshore Structures Congress (ISSC) gives an informative account of the reliability assessment of a mobile offshore unit [1] The reliability analyses reported start with the basic building block of a ship structure, the stiffened panel, and then progresses to the cross-section. Databases of basic variable uncertainty relating to geometry, material properties and environmental observations conducted over a number of years are described.

Modeling and methodological uncertainties were quantified by making use of test data and full scale measurements. The modeling uncertainties related to plate panel and stiffened panel component strengths while the methodological uncertainties related to systems such as the ship cross-section, the use of linear and non-linear strip theory, combinations of still water and wave bending stresses, etc. Structural reliability theory, if properly applied, enables naval architects and offshore engineers to deal with unavoidable modeling and methodological uncertainties in design and in-service assessment of marine structures in a fundamental manner.

This paper focuses on one important aspect of ship structure integrity, in-service defects. In recent years naval architects have been blamed by master mariners for the poor structural condition of merchant ships, particularly bulk carriers. Structural members in both aging and new ships are too often found to be severely corroded, cracked and dented. Structural reliability theory if applicable to these ships has to take full account of such defects. A time variant reliability method is applied to predict the long term failure probability of the mobile unit with a hypothetical corroded condition. A comparison between the current reliability prediction and that in [1] serves to highlight the detrimental effects of in-service defects on structural integrity. Every attempt is made to maintain the uncertainties used in the analysis in [1] so as to provide a common basis for comparison.

The vessel selected for analysis is not conventional. It is a mobile offshore unit for oil production and storage or oil tanker. It was primarily designed to operate in a turret moored mode with capabilities for two or multiple well risers. It has a helideck, 60 bed accommodation, three cranes, four gas turbines coupled to generators, and a general purpose process system. A dynamic positioning system is also available to facilitate heading control and to reduce peak mooring line loads on the turret system. The ship was assumed moored and always positioned heading into the predominant wind or wave direction. The vertical mooring forces are small and are considered to have an insignificant influence on the bending moment response. The vessel particulars for a full load operating condition are listed in Table 1. Figure 1.1 of [1] presents elevation and plan views of the vessel.

Load Assessment

Only vertical bending moment is considered, divided into still water-induced M_{sw} and wave-induced M_w components. In general, it is difficult to assess the degree of correlation between these two components. As a first

approximation they may be considered independent. Recent developments in probabilistic modeling of still water and wave-induced loads on ships hulls are presented in [2], [3].

Still Water Loads

The short-term still water bending stress σ_{sw} of the vessel was demonstrated in [4] to closely follow a Rayleigh distribution, see Figure 2.7 of [1] extracted from [4], therefore

$$F(\sigma_{sw}) = 1 - e^{-\sigma_{sw}^2/2B_{sw}^2} \qquad (1)$$

Principle dimensions		
Length between perpendiculars	L_{pp}	194.2 m
Molded breadth	B_m	32.0 m
Depth above baseline	D	16.0 m
Draught above baseline	T	10.0 m
Draught above keel		12.0 m
Displacement	Δ	50620 t
Midship section data		
Moment of inertia about horizontal axis	I_h	180.5 m4
Moment of inertia about vertical axis	I_v	474.5 m^4
Height of horiz. neutral axis above baseline		6.935 m

Table 1
Principle dimensions and particulars

For the present analysis, a value of 19.44 MPa was adopted for B_{sw} as found in [4].

Wave-Induced Loads

Vertical and horizontal hull girder bending moments in regular waves were calculated using linear strip theory [5]. The hull form was modeled with 28 unequally spaced sections. Two-dimensional hydrodynamic sectional properties were calculated with the Frank close-fit method [6].

Transfer functions for combined stress response at the upper deck corner in forward and bow incoming waves were calculated using the midship section moduli: 19.908 m^3 for vertical bending and 30.61 m^3 for horizontal bending. In bow waves, the phase lag between vertical and horizontal bending moments was taken into account. The transfer functions for combined stress, Figure 2.1 of [1], show that the highest stresses at an upper deck corner occur when the waves encounter the ship from the opposite side.

If H_s is significant wave height, T_z is the mean zero up-crossing period, and ω = wave frequency, the stress responses in short-term irregular long-crested seas were evaluated for the standard two-parameter Pierson-Moskowitz spectra according to

$$s_w(\omega) = \frac{H_s^2 T_z}{8\pi^2}\left(\frac{2\pi}{\omega T_z}\right)^5 e^{-\frac{1}{\pi}\left(\frac{2\pi}{\omega T_z}\right)^4} \qquad (2)$$

Non-linear contributions due to changes in buoyancy, added mass and damping during the motion of the ship increase the sagging bending moment by between 8 and 18% whereas the hogging moment decreases by between 15 and 17%. Assuming a symmetrical distribution around the linear result, a bias factor of 1.15 for the sagging moment and 0.85 for hogging seem appropriate for the extreme sea state. A standard deviation of 0.03 was adopted to account approximately for the spread in the results.

For further load and strength analysis, only the vertical bending distribution obtained from long-crested seas is applied. This gives approximately 7% higher levels than the distribution for short-crested seas. Comparisons with full scale measurements indicate a bias factor of 0.90 on the calculated values for long-crested seas. It is reasonable to believe that the major part of the bias is due to directional spreading.

Hull Girder Cross-Sectional Strength

For the cross-section reliability analysis, a simplified approach was chosen [7]. It is based on the observation that the ultimate moment capacity M_u of longitudinally framed hulls under vertical bending is closely correlated to the ultimate strength of the critical compression panel, as shown in Fig. 1 where M_p is the fully effective plastic moment. The hull girder ultimate strength model in [7] is summarized in Table 2.

Analysis of the girder under hogging and sagging in accordance with the Table 2 procedure was conducted. The results are listed in Table 3 from which it can be seen that deck panel no. 3 is the most critical one from the girder strength viewpoint although it is not the panel demonstrating the lowest panel strength.

Failure Equations and Probabilistic Modeling

The failure equation is

$$\chi_u M_u - \chi_{NL}\chi_{MC} Z \sigma_w - \chi_{sw} Z \sigma_{sw} \geq 0 \qquad (3)$$

where M_u is the ultimate bending moment evaluated as indicated in Table 2 and the remaining variables are as

1.	Determine the plastic neutral axis position of the fully effective section, i.e. the axis that divides the section into two parts with equal squash loads in compression and tension.
2.	Calculate the plastic moment M_P.
3.	Identify the critical stiffened panel. As a first attempt, select the panel appearing most frequently in the compression flange in either sagging or hogging. More precisely, calculate the cross-sectional strength for a number of stiffened panels to identify that producing the lowest ultimate moment.
4.	Compute values of the stiffened panel column slenderness λ and the plate panel slenderness β for the critical panel where $\lambda = (l/r\pi)\,(\sigma_y/E)^{0.5}$ $\beta = (b/t)\,(\sigma_y/E)^{0.5}$ l = length of stiffened panel r = radius of gyration of fully effective stiffened panel σ_y = yield stress (use weighted average of plate and stiffener yield stress based on areas) E = Young's modulus b = longitudinal stiffener spacing t = plating thickness
5.	Calculate the ultimate strength ratio φ of the critical panel $\varphi = \sigma_u/\sigma_y = (0.960 + 0.765\lambda^2 + 0.176\beta^2 + 0.131\lambda^2\beta^2 + 1.046\lambda^4)^{-0.5}$
6.	Calculate the ultimate bending moment ratio for the girder in sagging $M_{us}/M_p = -0.172 + 1.548\,\varphi - 0.368\,\varphi^2$ in hogging $M_{uh}/M_p = 0.003 + 1.459\,\varphi - 0.461\,\varphi^2$

Table 2
Hull Girder Strength Model in Hogging and Sagging

defined in Table 4 together with their adopted distribution functions.

The basis for the probabilistic modeling adopted for each of the variables is as follows:

- σ_y In this approach, the stiffened panel derivation considers adjacent half panels with alternate initial deformation modes. Thus strength is controlled by the combined failing of the plate in one panel and the stiffener in the other. The stiffened panel response is initially governed by loss of stiffness in the initially distorted plating but strength is then usually limited by the onset of yield at the stiffener tip. In [7] it was assumed in the derivation of the present formulation that the yield stresses in the plate and the stiffener were the same. The effect of different yield stresses has only been specifically examined in the course of conducting comparisons between test results and predictions. An average value weighted in accordance with the plate and stiffener areas was judged to be the most appropriate value for the present analysis;

- E,l,b,f,t_f,d_w,t_w,t_p modeled as in the corresponding committee work of ISSC'88 [8];

- σ_w based on the linear long-crested wave bending results determined above;

- σ_{sw} as determined above;

- χ_u this value may be assessed by means of experimental-calculation comparisons. This was conducted [7] leading to a bias of 1.018 and COV of 0.061. The tests involved a small number of laboratory tests on steel box girders. These are not necessarily fully representative of ships girders so the COV was increased to 0.15, a compromise between the derived value and that of 0.20 suggested in [9];

- χ_{NL} the effects of non-linearity were described above. The bias found is in good agreement with that proposed in [10], namely, bias = $1.74 - 0.93C_B$ where C_B is the block coefficient - the agreement is acceptable considering that this equation was determined from scarce experimental data available on non-linear ship response. The standard deviation adopted is also similar to that found in [10];

- χ_{MC} this was evaluated from an analysis of the relevant full scale data as described in [1]. The factor accounts for the uncertainties arising from spectral representation and from the shape of the transfer function which is usually predicted using linear strip theory. The model uncertainty, normally distributed with a bias of 0.90 and standard deviation of 0.135, is in good agreement with the formulation in [10], namely,

Panel		Stfnr + Plate	r (m)	t (mm)	b (m)	$\sqrt{(\sigma_y/E)}$	λ	β	φ	M_U/M_p
Deck	1	1	.088	18.5	0.810	.0391	0.523	1.711	0.731	0.762
		2	.087	17.5	0.850	.0391	0.529	1.900	0.702	0.733
		3	.085	18.5	0.900	.0391	0.541	1.902	0.698	0.729
	2	1	.078	14.5	0.690	.0391	0.585	1.860	0.688	0.718
	3	1	.0795	13.5	0.690	.0391	0.579	1.990	0.679	0.709
	4	1	.0935	13.5	0.690	.0391	0.492	1.990	0.702	0.733
Bottom	1	1	.1399	10.5	0.725	.0391	0.329	2.700	0.640	0.747
		2	.1392	10.5	0.750	.0391	0.331	2.792	0.627	0.736
	2	1	.1387	10.5	0.670	.0391	0.332	2.494	0.668	0.772
	3	1	.1382	10.5	0.690	.0391	0.333	2.569	0.657	0.762
	4	1	.1382	10.5	0.690	.0391	0.333	2.569	0.657	0.762
	5	1	.1341	13.5	0.756	.0391	0.343	2.189	0.710	0.806
	6	1	.0680	18.0	0.500	.0391	0.677	1.086	0.743	0.832
	7	1	.1382	10.5	0.690	.0391	0.333	2.569	0.657	0.762

Table 3
Deck and Bottom Stiffened Panel Strength and Girder Ultimate Moment

$$\text{bias} = -0.0050\theta + 0.42V + 0.70C_B + 1.25 \quad 90° \le \theta \le 180°$$

$$\text{bias} = -0.0063\theta + 1.22V + 0.66C_B + 0.06 \quad 0° \le \theta \le 90°$$

and a standard deviation is 0.12 where θ is heading in degrees (180° corresponding to head waves) and V is Froude number. These equations have been determined by a systematic comparison between theoretical and experimental results;

- χ_{sw} derived from the data in [4];

- H_s,T_z these were determined as the most likelihood fits to the wave scatter diagram in [1], H_s being based on a 3-parameter Weibull distribution and T_z on a lognormal distribution;

- α 0.1 mm/ yr is a typical rate adopted by classification societies although normally the COV can be expected to be 100%. Vessels with inadequate maintenance which result in accelerated corrosion effects may be declassed in respect of 'corrosion control'. In these cases, rates approaching 0.2 mm/yr are more typical. The rate in the webs and flange plates was taken as twice the basic value adopted for the attached plating.

Time Variant Reliability

The long term probability of the overall load effects exceeding a degraded strength threshold depends on random parameters grouped into three categories, i.e. slowly varying random variables Q, time invariant random variables R, and stochastic load processes $Z(\tau)$. The variables Q may be the seastate parameters (e.g. significant wave height and mean zero crossing period of, typically, three hours duration) and still water load effects the duration of which is equal to that of the voyage. The R variables include those describing material properties, corrosion rates, modeling uncertainties of the limit state equations and the statistical uncertainties of the seastate parameters. The processes $Z(\tau)$ are the wave induced components. Figure 1 of [11] illustrates the durations of these various random variables.

If the seastates are assumed independent of each other, the long term probability $P_f(t)$ can be expressed by

$$P_f(t) = 1 - (1 - P_{f0})\, E_R \prod_{k=1}^{n_{voy}} \times$$

$$E_{Q_{sea}} \left[\prod_{j=1}^{n_k} E_{Q_{sea}} \left\{ \exp\left[-\nu^+_{kj}(\tau_{kj})\, \Delta\tau_{kj} \right] \right\} \right] \qquad (4)$$

where

P_{f0} is the initial probability

$\nu^+_{kj}(\tau_{kj})$ is the mean outcrossing rate from the safe domain of the limit state equation into its failure domain at time τ_{kj}

Variable	Description	Distribution Type	Mean Value	COV
σ_y	Yield stress	Lognormal	392	0.066
E	Young's modulus	Normal	210,000	0.05
l	Panel length	Normal	3700	0.04
b	Panel width	Normal	690	0.04
f	Stiffener flange width	Normal	90	0.04
t_f	Flange thickness	Normal	15	0.04
d_w	Web height	Normal	250	0.04
t_w	Web thickness	Normal	10.0	0.04
t_p	Plate thickness	Normal	13.5	0.04
σ_w	Wave bending stress	N. process	0.0	Sea state dep.
σ_{sw}	Still water bending stress	Rayleigh	24.36	0.523
χ_u	Strength modulus uncertainty	Normal	1.0	0.15
χ_{NL}	Non-linear correction	Normal	1.15	0.026
χ_{MC}	Measured versus calculated	Normal	0.90	0.15
χ_{sw}	Still water modulus uncertainty	Normal	1.0	0.05
H_s	Significant wave height	Weibull	-	-
T_z	Zero crossing period	Lognormal	-	-
α	Corrosion rate	Lognormal	0.1 - 0.2	0.5 - 1.0
Z	Elastic section modulus	Determ.	19.91	-
Z_p	Plastic section modulus	Determ.	28.00	-
D	Duration	Determ.	0-20	-
α_z	Plastic section modulus reduction rate	Lognormal	0.01 - 0.02	0.5 - 1.0
Stresses = MPa, dimensions = mm, corrosion rate = mm/yr, section modulus = m^3, duration = year				

Table 4
Variable Probabilistic Modeling for Approach 1

$\Delta\tau_{kj}$ is the time interval of the *j*th seastate in the *k*th voyage

n_k is the total number of sea states in the k^{th} voyage

n_{voy} is the total number of voyages during the period (0,t)

Q_{sea} are the seastate parameters

Q_{kst} are the still water load effects at the k^{th} voyage.

Normally, a marine unit undergoes several loading conditions such as homogeneously loaded, deep water ballast, etc. Variable Q_{kst} belongs to the still water load effects of one of these load conditions. For each load condition, the variables Q comprise the seastate parameters Q_{sea} and the still water load effects.

Direct numerical calculation of the above equation is not feasible, and it is always helpful to estimate the lower and upper bounds on $P_f(t)$ by

$$P_f(t) \geq P_{fl}(t) = 1 - (1 - P_{f0}) \times$$

$$E_R\left[\prod_{i=1}^{m} E_{Q_i}\left\{\exp\left[-\gamma_i N_i^+(t)\right]\right\}\right] \qquad (5a)$$

$$P_f(t) \leq P_{fu}(t) = 1 - (1 - P_{f0}) \times$$

$$E_R\left[\prod_{i=1}^{m} \exp\left\{-\gamma_i E_{Qi}\left[N_i^+(t)\right]\right\}\right] \qquad (5b)$$

$$P_{ful}(t) \le P_{fu2}(t) = 1 - (1 - P_{f0}) \times \exp\left[-\sum_{i=1}^{m} \gamma_i \, E_{(R+Q)i}\left[N_i^+(t)\right] \right] \qquad (5c)$$

where

γ_i is the mean percentage of time during which the structure is in the i^{th} load condition;

m is the total number of load conditions;

$N_i+(t)$ is the conditional mean outcrossing number within a time period (0,t) in the i^{th} load condition.

Although eqns (6a) and (6b) can provide lower and upper bounds on $P_f(t)$, their calculation requires the solution to multi-level integral problems. The scope of difficulty can be envisaged.

However, estimates of the lower and upper bounds on $P_f(t)$ can be calculated by using the asymptotic Laplace integration technique. The theory is documented in many references such as [12]. Its potential application to structural reliability analysis is discussed in some detail in [13]. What is more significant is that past asymptotic reliability analysis methods are found to be related directly to and can be explained by this technique.

The concept of maximum likelihood can be more clearly illustrated by application of the method. The lower and upper bounds to $P_f(t)$ require the following asymptotic results.

Estimation of $P_{fu2}(t)$ and its Sensitivity Factors

The solution of eqn (6c) can be easily obtained if the mean outcrossing number $E_{(R+Q)i}[N_i(t)]$ is known. Frequently,the generalized safety index is widely quoted to compare relative structural safety. Following this convention, ß(t) denotes the safety index given by

$$\beta(t) = -\Phi^{-1}\left[P_{fu2}(t)\right] \qquad (6)$$

The sensitivity factors of the estimated long-term probability of exceedance $P_{fu2}(t)$ to changes in distribution parameter values are also calculated based on the asymptotic Laplace integration technique. Here the effects of changes in the distribution parameter Θ on P_{f0} are not included because it is small compared with $P_{fu2}(t)$. The sensitivity factors are therefore given by

$$\frac{\delta\beta(t)}{\delta\Theta} = -\frac{\Phi[\beta(t)]}{\varphi[\beta(t)]} \sum_{i=1}^{m} \gamma_i \frac{\delta E_{(R+Q)_i}\left[N_i^+(t)\right]}{\delta\Theta} \qquad (7)$$

However, this equation becomes invalid when the long term probability $P_{fu2}(t)$ is high. In this case, the asymptotic Laplace integration technique gives poor estimates of $P_f(t)$ and even worse estimates of the sensitivity factors.

Estimation of P_{f0}

The initial probability P_{f0} is relatively small compared with $P_f(t)$ and only gives an indication of the initial stress state of the structure. If the random variables involved are denoted as $X = \{R,Q,Z(\tau)\}$ with a total number of random variables n_X, the analytical expression of the initial probability P_{f0i} in the *i*th load condition is

$$P_{f0i} = \int_{F_i} f_{x_i}(x)\, dx = \int_{F_i} \exp[l_{x_i}(x)]\, dx\,, \quad l_{x_i}(x) = \ln f_{x_i}(x) \qquad (8)$$

where

F_i is the integration domain at time $\tau = 0$ and contains the area enclosed by the limit state equation $g(X,\tau) \le 0$ and bounds on random variables X;

$f_{Xi}(X)$ is the joint density function of X;

$g(X,\tau)$ is the limit state equation.

The initial failure probability P_{f0} for these exclusive load conditions is given by

$$P_{f0} = \sum_{i=1}^{m} \gamma_i P_{f0i} \qquad (9a)$$

$$P_{f0i} \times \frac{\sqrt{(2\pi)^{n_x - p_x}}\, f_{x_i}(X^*)}{\prod_{q=1}^{p_x} \lambda_{x_q} \sqrt{|\det(A_x^T A_x)|\, |\det[A_x^{*T} H_{x_i}(x^*)\, A_x^*]|}} \qquad (9b)$$

$$H_{x_i}(X^*) = \left[\frac{\partial^2 l_{x_i}(X^*)}{\partial x_k \partial x_j} - \lambda_{x_i} \frac{\partial^2 g(X^*,\tau)}{\partial x_k \partial x_j} \right]_{k,j=1,\ldots,n_x} \qquad (9c)$$

$$\left\{\lambda_{x_q}\right\}^T_{Q=1,\ldots,p_x} = (A_x^T A_x)^{-1} A_x^T \nabla X\, l_{x_i}(X^*) \qquad (9d)$$

where

A_XT is a p_X x n_X matrix with its first row equal to $\nabla X\, g(X^*,\tau)/|\nabla X\, g(X^*,\tau)|$ at $\tau = 0$ and with the rest of the rows equal to the derivatives of the active bounds;

p_X is the total number of active constraints

A_X^* is a n_X x (n_X - p_X) matrix the (n_X - p_X) vectors of which form an orthonormal basis of the subspace orthogonal to the subspace spanned by the p_X vectors in A_X.

The value of X* is obtained from the following minimisation

$$\min -\ln f_{xi}(X) \text{ for } x \in \{g(X,\tau) \le 0,\ X_{min} \le X \le X_{max}\} \quad (10)$$

in which X_{min} and X_{max} are the lower and upper bounds on X respectively.

Estimation of $E_{(R+Q)i}[N_i^+(t)]$ and its Sensitivity Factors

Analytically the mean outcrossing number $E_{(R+Q)i}[N_i^+(t)]$ can be expressed as a standard volume integral as follows:

$$E_{(R+Q)i}[N_i^+(t)] = \int_0^T \int_{\dot{F}_i} \Psi(X,\tau)\ \mathrm{Tr}(X,\tau) \exp[l_{x_i}(X)]dy \quad (11a)$$

$$dX = \{R,Q,Z(\tau)\}^T,\quad Y = \{z_2,\ldots,z_{n_z},R,Q,\tau\}^T \quad (11b)$$

$$\Psi(X,\tau) = \sigma_{\dot{z}_n}\left[\Phi\left(\frac{\dot{F}_n - \mu_{\dot{z}_n}}{\sigma_{\dot{z}_n}}\right) - \left(\frac{\dot{F}_n - \mu_{\dot{z}_n}}{\sigma_{\dot{z}_n}}\right)\Phi\left(\frac{\dot{F}_n - \mu_{\dot{z}_n}}{\sigma_{\dot{z}_n}}\right)\right] \quad (11c)$$

$$\dot{F}_n = \frac{\partial g(X,\tau)/\partial\tau}{|\nabla Z\, g(X,\tau)|},\quad n(X,\tau) = \frac{\nabla Z\, g(Z,\tau)}{|\nabla Z\, g(X,\tau)|} \quad (11d)$$

$$\mu_{\dot{z}n} = n^T(X,\tau)\, C_{\dot{z}z}\, C_{zz}^{-1}\,(Z - \mu_z) \quad (11e)$$

$$\sigma_{\dot{z}_n^2} = n^T(X,\tau)\,(C_{\dot{z}\dot{z}} - C_{\dot{z}z}\, C_{zz}^{-1}\, C_{\dot{z}})\, n(X,\tau)$$

where

$\dot{F}_i$ is the domain by the lower and upper bounds on Y in the i^{th} load condition;

$\dot{F}_n$ represents the normalized rate of deterioration of the limit state surface;

$\dot{Z}_n$ is the projection of $\dot{Z}(\tau)$ on n(X, τ);

μ_z is the mean value vector of $Z(\tau)$.

The above equations use the covariance matrix for $\{Z(\tau), \dot{Z}(\tau)\}$ given by

$$C_{[Z,\dot{Z}]} = \begin{pmatrix} C_{zz} & C_{z\dot{z}} \\ C_{\dot{z}z} & C_{\dot{z}\dot{z}} \end{pmatrix}$$

The asymptotic solution to eqn (12a) is derived in a similar manner as for eqn (9)

$$E_{(R+Q)i}[N_i^+(t)] \times \frac{\sqrt{(2\pi)^{n_x - p_y}}\,\Psi(X^*,t)\ \mathrm{Tr}(X^*,t) F_{x_i}(X^*)}{\prod_{q=1}^{P_y} \lambda_{y_q} \sqrt{|\det(A_y^T A_y)|\ |\det[A_y^{*T} H_{y_i} A_y^*]|}} \quad (12a)$$

$$\frac{\partial z_1}{\partial y_k} = -\frac{\partial g(X^*,t)/\partial y_k}{\partial g(X^*,t)/\partial z_1},\quad H_{y_i} = \{B_{kj}\}_{k,j=1,\ldots,n_x} \quad (12b)$$

$$B_{kj} = \frac{\partial^2 l_{x_i}(X^*)}{\partial y_k \partial y_j} + \frac{\partial^2 l_{x_i}(X^*)}{\partial y_k \partial z_1}\frac{\partial z_1}{\partial y_j} + \frac{\partial^2 l_{x_i}(X^*)}{\partial y_j \partial z_1}\frac{\partial z_1}{\partial y_k} + \frac{\partial l_{x_i}(X^*)}{\partial z_1^2}\frac{\partial z_1}{\partial y_k}\frac{\partial z_1}{\partial y_j} + \frac{\partial l_{x_i}(X^*)}{\partial z_1}\frac{\partial^2 z_1}{\partial y_k + \partial y_j} \quad (12c)$$

$$\frac{\partial^2 z_1}{\partial y_k \partial y_j}\frac{\partial g(X^*,t)}{\partial z_1} = -\frac{\partial^2 g(X^*,t)}{\partial y_k \partial y_j} - \frac{\partial^2 g(X^*,t)}{\partial y_k \partial z_1}\frac{\partial z_1}{\partial y_j} - \frac{\partial^2 g(X^*,t)}{\partial y_j \partial z_1}\frac{\partial z_1}{\partial y_k} - \frac{\partial^2 g(X^*,t)}{\partial^2 z_1}\frac{\partial z_1}{\partial y_k}\frac{\partial z_1}{\partial y_j} \quad (12d)$$

$$\{\lambda_{y_q}\}_{q=1,\ldots p_y} = (A_y^T A_y)^{-1} A_y^T \nabla Y\, l_{x_i}(X^*) \quad (12e)$$

where

$A_Y T$ is a p_Y x n_X matrix with its first row equal to the derivatives of the active constraints including the time constraint τ = t but excluding the limit state equation;

p_Y is the total number of active constraints;

A_Y^* is a n_X x (n_X - p_Y) matrix the (n_X - p_Y) vectors of which form an orthonormal basis of the subspace orthogonal to the subspace spanned by the p_Y vectors in A_Y.

The value of X* is obtained from the following minimisation

$$\min -\ln f_{xi}(X) \text{ for } x \in \{g(X,t) \le 0,\ X_{min} \le X \le X_{max}\} \quad (13)$$

as in most cases, the most likely outcrossing point X* is obtained at time τ = t when the strength-degraded structure retains its lowest strength. For any statistical parameter describing the distribution function, the sensitivity factor can be obtained from

$$\frac{\partial E_{(R+Q)i}[N_i^+(t)]}{\partial \Theta} \times E_{(R+Q)i}[N_i^+(t)]\frac{\partial l_{x_i}(X^*)}{\partial \Theta} \quad (14)$$

As Θ is not present in the limit state equation g(X,τ), it only affects the value of $l_{Xi}(X)$.

A much simpler solution to $E_{(R+Q)i}[N_i(t)]$ can be obtained if the original random variables are mapped onto a set of

standard normal variables and curvature effects of the limit state equation are not considered. This solution is

$$E_{(R+Q)i}\left[N_i^+(t)\right] = \frac{\varphi(\beta)}{\beta}\frac{\sigma_{\dot{z}_n}}{\dot{F}_n} \times \left[\varphi\left(\frac{\sigma_{\dot{z}_n}}{\dot{F}_n}\right) - \left(\frac{\dot{F}_n}{\sigma_{\dot{z}_n}}\right)\Phi\left(-\frac{\sigma_{\dot{z}_n}}{\dot{F}_n}\right)\right] \quad (15)$$

where

$\dot{F}_n$, $\sigma_{\dot{z}_n}$ are calculated using eqns (12c) and (12d) in the transformed variable space;

ß is the distance from the origin of the transformed variable space to the most likely outcrossing point.

Estimation of $P_{fl}(t)$ and $P_{ful}(t)$

The lower and narrower upper bounds expressed by eqns (6a) and (6b) have to be determined by the nested reliability method. The fundamental concept of this method is well reported (14) (15) (16). So far, the nested reliability method based on FORM has normally been used although, in principle, any reliability algorithm can be incorporated at the expense of having to determine higher order derivatives. However, it should be noted that the accuracy of the nested reliability method by FORM may be undermined by the errors accumulated in a FORM analysis (17). A slightly different solution scheme has been proposed in (18) based on a multiple objective minimisation strategy. If $P_{ful}(t)$ is sought, the following formulation is required.

Given a set of values of $r \in R$, it is always possible to estimate the conditional probability $P_{ful}(t|r)$. The unconditional probability $P_{ful}(t)$ is written hereafter as

$$P_{ful}(t) = \int P_{ful}(t|r)\, f_r(r)dr = P[g_1(u_a,R) \le 0] \quad (16a)$$

in which u_a is an auxiliary standard normal variable and

$$g_1(u_a, R) = \Phi(u_a) - P_{ful}(t|R) \quad (16b)$$

The original problem is then reduced to the following objective minimisation calculation

$$\min_{W,\,u_a} \| W, u_a \|$$

$$\min_{Q,\,Z} -\ln f_{q,z}(Q, Z) \quad (17)$$

$$g_1(W, u_a) \le 0$$

$$g(W, Q, Z) \le 0$$

where

W denotes the transformed standard normal variables of R;

$f_{Q,Z}(Q,Z)$ is the joint probability density function.

The approximation to $P_{ful}(t)$ in the end can be given as

$$P_{ful}(t) = \Phi(-\|W,u_a\|) \quad (18)$$

A similar strategy can be adapted to determine $P_{fl}(t)$.

Results

The analysis was first conducted assuming full corrosion control, i.e. no corrosion, to determine consistency of the results with those obtained by ISSC Committee V.I. This condition is designated Condition A. Three combinations of corrosion rate and its variability were then evaluated, designated Conditions B, C, and D. The combinations of corrosion rates and variabilities were as follows:

Condition	α		α_z	
	mean (mm/yr)	COV	mean (1/yr)	COV
A	0.0	0.0	0.00	0.0
B	0.1	0.5	0.01	0.5
C	0.1	1.0	0.01	1.0
D	0.2	0.5	0.02	0.5

The variation in safety index with service life for each of these conditions is presented in Figure 2. As expected, as the rate and degree of uncertainty of the corrosion rate increase, so does the failure probability. Initially, however, the effect of corrosion is minimal. For the lower mean rates (Conditions B and C), the effect of corrosion on girder strength reliability is not influential for some 10 years. For the higher rate, Condition D, it is 5 years. With no effective maintenance, Condition D leads within 10 to 15 years to vessels with failure probabilities approaching 1 in 10.

The solutions for Conditions B to D were derived using eqn (17) which include the time variant capability. Being an asymptotic solution, it is not expected to be accurate for service lives of short duration during which corrosion is negligible. Condition A was evaluated using eqn (5) assuming a mean outcrossing rate independent of time. It is therefore accurate across the complete range of lives. Thus, for service lives of short duration, the asymptotic solutions will not converge to the Condition A result because of the use of different algorithms in realizing these solutions. The major advantage of the multiple objective minimisation technique is that it eliminates the

iterations required of nested reliability analyses. Thus, a major computational advantage is realized with this technique.

The most likely failure points for each of these cases assuming 20 years of exposure are listed in Table 5 together with the 100 year result for Condition A. With the corrosion free condition, generally only the time dependent variables (bending stresses, wave height, etc) demonstrate different values at the most likely failure points. With the introduction of corrosion, the failure point moves to a different part of the failure domain, the extent of the move dependent upon the sensitivity of the system to the variable and, in turn, a function of its inherent variability. The variables most prominent in this respect are wave bending stress, significant wave height, strength modeling uncertainty, and wave calculation accuracy.

Variable	Condition (Service life)				
	A (100 yr)	A (20 yr)	B (20 yr)	C (20 yr)	D (20 yr)
σ_w	118.2	101.4	76.87	75.93	80.44
σ_{sw}	69.00	81.51	87.75	83.76	76.72
H_s	12.97	12.16	11.00	10.85	11.21
T_z	11.43	11.09	10.58	10.50	10.67
σ_y	379.1	379.1	385.3	389.3	390.4
E	207800	207800	208600	209600	209800
I	3707	3707	3710	3704	3702
b	696.1	696.1	694.3	691.2	690.9
f	89.90	89.90	89.94	89.98	89.98
t_f	14.98	14.98	14.98	15.00	15.00
d_w	248.8	248.8	249.3	249.8	249.9
t_w	9.999	9.999	9.998	9.999	9.999
t_p	13.40	13.40	13.42	13.48	13.49
χ_u	0.577	0.553	0.836	0.956	0.977
χ_{NL}	1.156	1.155	1.152	1.151	1.150
χ_{MC}	1.030	1.017	0.958	0.919	0.911
χ_{sw}	1.009	1.011	1.007	1.002	1.001
α	-	-	0.1050	0.0787	0.1966
α_z	-	-	0.0166	0.0235	0.0196

Table 5
Values of the Basic Variables at the Most Likely Failure Point

Comparison between the above corrosion free results and the equivalent results presented in [1] demonstrates that they are in general agreement. Differences are to be expected because of the different algorithms adopted to execute the assessments.

Conclusion

The effect of corrosion on the likelihood of ultimate girder failure has been examined using a reliability procedure based on the multiple objective minimisation technique. The example considered is the floating production unit analyzed in some detail in the 1991 ISSC report by Committee V.I. However, as pointed out during the discussion at the Congress, the Committee report did not take account of the effects of corrosion. It is hoped the presented work goes some way to compensate for this.

References

1. Report of Committee V.I., "Applied Design," Proceedings of the 11th International Ship and Offshore Structures Congress, Volume 2, Edited by P.H. Hsu and Y.S. Wu, Elsevier Applied Science, London 1991.
2. Guedes Soares, and Moan, Trans. Society of Naval Arch. and Marine Engineers, Vol. 96, 1988, pp. 129-156.
3. Guedes Soares, Structural Safety, Vol. 8, 1990, pp. 353-368.
4. Moan, T. and Jiao, G., "Characteristic Still Water Effects for Production Ships," University of Trondheim, December 1988.
5. Salvesen, Tuck and Faltinsen, SNAME Transactions, Vol 78, 1970.
6. Frank, W., "Oscillation of Cylinders in or Below the Free Surface of Des," NSRDC Report 2375, 1967.
7. Frieze, P.A. and Lin, Y-T., "Ship Longitudinal Strength Modeling for Reliability Analysis," Proceedings Marine Structural Inspection, Maintenance and Monitoring Symposuim, SSC/SNAME, Arlington, March 1991.
8. Report of Committee V.I., "Applied Design," Proceedings, 10th International Ship and Offshore Structures Congress, Vol. 2, Technical University of Denmark, Lyngby, 1988.
9. Faulkner, D., oral discussion to Report of ISSC'88 Committee V. 1, Lyngby, August, 1988

10. Guedes Soares, C. and Moan, T., "Uncertainty Analysis and Code Calibration on the Primary Load Effects in Ship Structures," ICOSSAR '85, 4th International Conference on Structural Safety and Reliability, 1985.

11. Shi, W.B., "Load Combinations by Log-Likelihood Maximization," in Practical Design of Ships and Mobile Units, Edited by J.B. Caldwell and G. Ward, Elsevier Applied Science, London, Vol 2, pp. 2.953-2.965.

12. Bleinstein, N. and Handelsman, R., "Asymptotic Expansions of Integrals," Dover, New York, 1986.

13. Breitung, J. of Eng. Mech., Vol. 117, No. 3, 1991.

14. Madsen and Tvedt, J. of Eng. Mech., Vol. 116, No. 10, 1990.

15. Fujita, M., Schall, G. and Rackwitz, R., "Time Variant Component Reliabilities by FORM/SORM and Updating by Importance Sampling," Proceedings 5th International Conference on Appl. of Statistics and Probability in Civil Engineering, Vancover, 1987.

16. Wen and Chen, Prob. Eng. Mech., Vol. 2, 1987, pp. 156-162.

17. Ronold, J. of Eng. Mech., Vol. 117, No. 9, 1991.

18. Shi, Marine Structures, Vol. 4, No. 5, 1991, pp. 435-453.

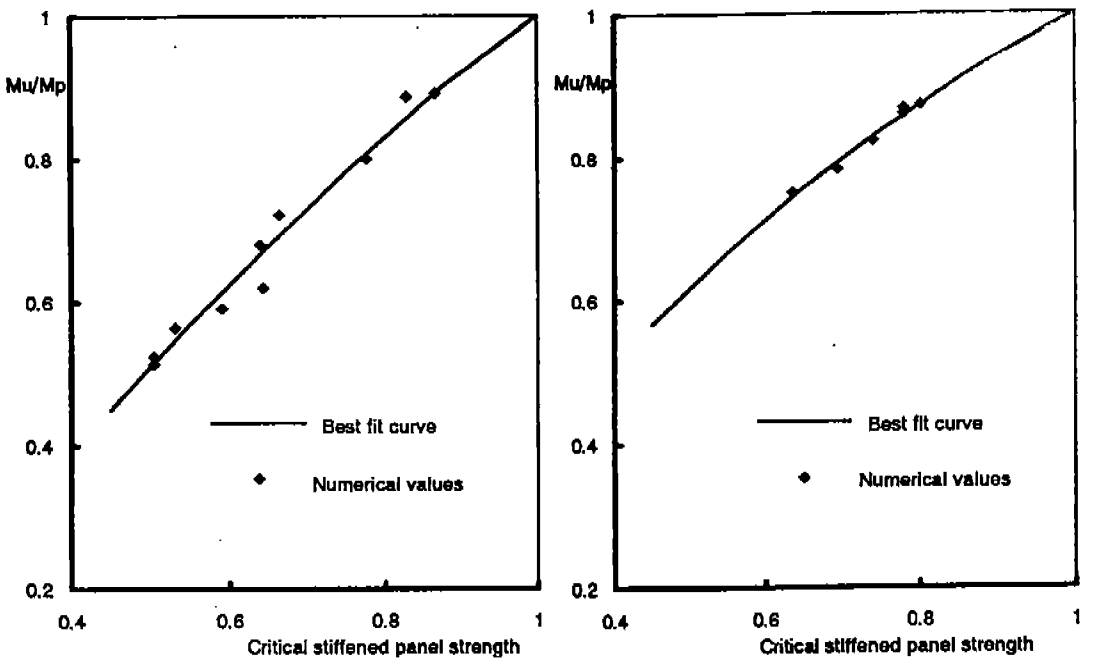

(a) Hull in Sagging

(b) Hull in Hogging

Figure 1
Ultimate Bending Moment versus Critical Panel Strength

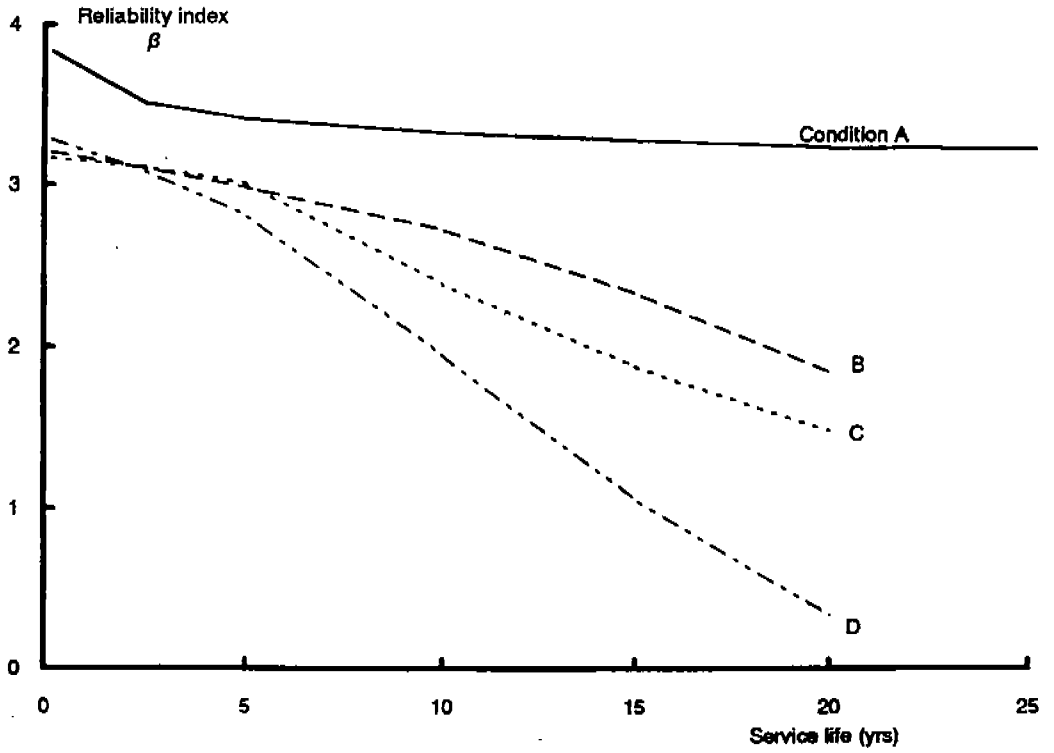

Figure 2
Effect of Corrosion on Service Life Reliability